A NOVEL BIO-INSPIRED MICROSTRUCTURE FOR PROGRESSIVE COMPRESSIVE FAILURE IN MULTIDIRECTIONAL COMPOSITE LAMINATES

Torquato, Garulli[a], Emile S., Greenhalgh[a], Silvestre T., Pinho[a]

a: Faculty of Engineering, Imperial College London, UK – t.garulli@imperial.ac.uk

Abstract: *In this study we take inspiration from biological materials to design a modified microstructure for laminated multidirectional (MD) carbon fiber reinforced polymers (CFRP), with the objective of mitigating their compressive failure behavior. We introduce soft inclusions in the form of thin longitudinal strips of foam in 0° load bearing layers, aiming at arresting kinkband propagation. We conceived a bespoke stacking sequence and developed a tailored procedure for manufacturing the microstructure. We then performed in-situ tests on small scale notched specimens from a baseline laminate and a modified one. Results are presented and discussed.*

Keywords: Bioinspiration; Compression; Damage diffusion; Microstructural design

1. Introduction

Longitudinal compressive failure is a major concern for CFRP. In most high-performance unidirectional (UD) composites, failure occurs by fiber kinking. In regions of fiber misalignment, the matrix undergoes shear, leading to further fiber rotation. With increasing load, either this mechanism becomes unstable, or shear fracture of the matrix/interface occurs, leading to unstable collapse and to kinkband formation [1]. In MD laminates, the failure process is more complex and may involve delamination and some progressive damage in the off-axis plies [2]. However, almost inevitably, sudden compressive fracture of load bearing (0°) layers is the final event leading to catastrophic failure, with negligible detectable warning. These complexities lead to a lack of strategies to mitigate the failure process and improve performance.

In this work, we take inspiration from nature to design a novel microstructure for MD CFRP laminates. Several biological materials present alternating stiff and soft zones. The associated periodic stiffness variations are an effective strategy to enhance fracture resistance: a strong decrease in crack driving force occurs when the crack propagates from stiff to soft regions, eventually leading to crack arrest [3]. To replicate such a condition in a MD laminate undergoing compression, we modified its microstructure by replacing continuous 0° composite layers with alternating of stiff (0° composite) and soft (polymethacrylimide -PMI- foam) longitudinal strips, Figure 1, with the objective of creating regions where kinkbands may be arrested, favoring 0° composite strips to fail individually and independently, due to the soft strips isolating them.

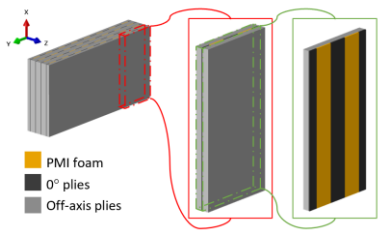

Figure 1. Simplified representation of the devised concept.

2. Material and methods

2.1 Materials

Since the soft inclusions are not load-bearing, a material with low specific weight is preferable for the soft inclusions. This, along with processing ease and compatibility, led to PMI foams being identified as optimal materials. PMI foam sheets, 0.07 mm thick, were provided by YoneshimaFelt Co. Ltd. Specifically, Rohacell® 200SL foam was used for this study (Table 1). The sheet thickness was chosen by considering commercial availability and compatibility in the design process.

Table 1: Rohacell® 200SL properties from [3].

Density [g/cm^3]	Tensile Modulus [MPa]	Compressive modulus [MPa]	Shear modulus [MPa]
0.205	371	370	123
	Tensile strength [MPa]	Compressive strength [MPa]	Shear strength [MPa]
	10.4	9.6	4.8

A 15gsm MR70/TP402 prepreg, commercially available from North Thin Ply Technologies (NTPT), was selected for this study. MR70 is a high-performance intermediate modulus carbon fiber; TP402 is a 135 °C curing epoxy used for automotive and aerospace applications. Properties for this material are not readily available from open literature, so, for the purpose of this study, they were estimated using micromechanics or assumed, as reported in Table 2 (with the standard notation used in [1]).

Table 2: MR70/TP402 properties.

Density [g/cm^3]	E_1 [GPa] (compressive)	E_2 [GPa]	G_{12} [GPa]	ν_{12}
1.55	153.	9.5	3.16	0.26
X_t [MPa]	X_c [MPa]	Y_t [MPa]	Y_c [MPa]	S_L [MPa]
3880.	1800.	39.	160.	60.

2.2 Configuration design

To test the concept, we developed a bespoke stacking sequence to be used as a baseline, which we called Baseline-No-Foam (BNF), and a modified version for the new microstructure, named Foam Laminate (FL). The two laminate stacking sequences are as follows:

- BNF: $[\pm 45/(\pm 75/90/\pm 75/\pm 31_9/0)_{S2}]_S$
- FL: $[\pm 45/(\pm 75/90/\pm 75/\pm 31_9/0_{2F})_{S2}]_S$. Here the subscript F indicates the presence of the foam strips in the 0° layers

The BNF laminate was designed to have elastic properties similar to those of a commonly used industrial reference laminate (i.e. $[(\pm 45/0/\pm 45/90/0)_n]_S$) and to contain a reduced number of 0°

layers. Also, the high number of ±31 layers was tailored to provide a strong support to the laminate at failure of the 0° layers. The FL sequence is obtained from the BNF one by doubling the number of 0° layers. In this case, however, 0° layers are intended as containing foam strips. Specifically, considerations of effectiveness and manufacturability led to the choice of having alternated 1 mm wide 0° composite and foam strips. Therefore, the BNF and FL laminates contain the same volume of composite material (and in the same orientations), the FL one being slightly thicker due to the presence of the foam.

2.3 Manufacturing

Prepreg sheets of the desired orientations were cut with a Blackman and White Genesis 2300 cutting machine. The BNF laminate was laid up manually according to standard practices. To prepare materials for the FL laminate, an Oxford Lasers Diode Pumped Solid State (DPSS) micro-machining system was used as follows:

- 0° prepreg layers, after being laid up in groups of four, $[0_4]$, were cut to have 1 mm wide rectangular slots in the fiber direction
- Foam sheets were cut, in their central region, to be divided into 1 mm wide strips
- PET sheets (125 µm thick) were cut to create templates for positioning of both the 0° prepreg layers and the foam strips

Lay-up of the foam laminate followed standard practices until each of the $[0_4]$ blocks, expected to contain foam strips, was reached; at this point a tailored procedure, exploiting the PET templates and involving multiple steps, was used to create the layer containing the foam strips. More in detail, the strips of 0° prepreg were laid first; afterwards, the foam strips were placed in the slots in between the prepreg. Figure 2 shows three stages of the process.

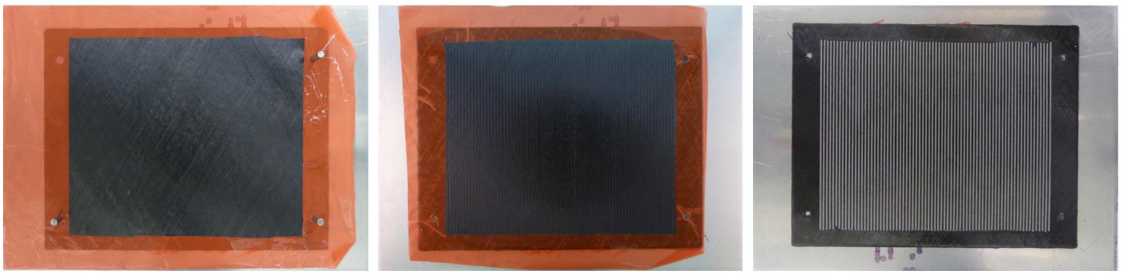

Figure 2. Three phases of the foam laminate lay-up procedure: (a) right before laying up a $[0]_4$ block containing the foam strips, (b) after laying up 0° prepreg strips, (c) after having laid up both prepreg and foam strips.

For this study, two small scale notched specimens for compression loading, Figure 3, were obtained from each of the two plates. The top and bottom faces of the specimens were ground parallel to ensure optimal loading during compression, while the notch was obtained by means of a disk saw; notch tip radius was found to be, by means of optical microscopy, consistently around 40-50 µm, figure 3 (c).

Due to an incident during manufacturing, the specimens' surface had to be slightly ground, which partially reduced their thickness (about 0.2 mm per specimen) and thus slightly modified their layup (by eliminating outer layers); this may have introduced some variability in the test

performed, but is not expected to have affected the qualitative observations presented here. Table 3 shows the ligament section dimensions and notch tip radii for the four specimens tested.

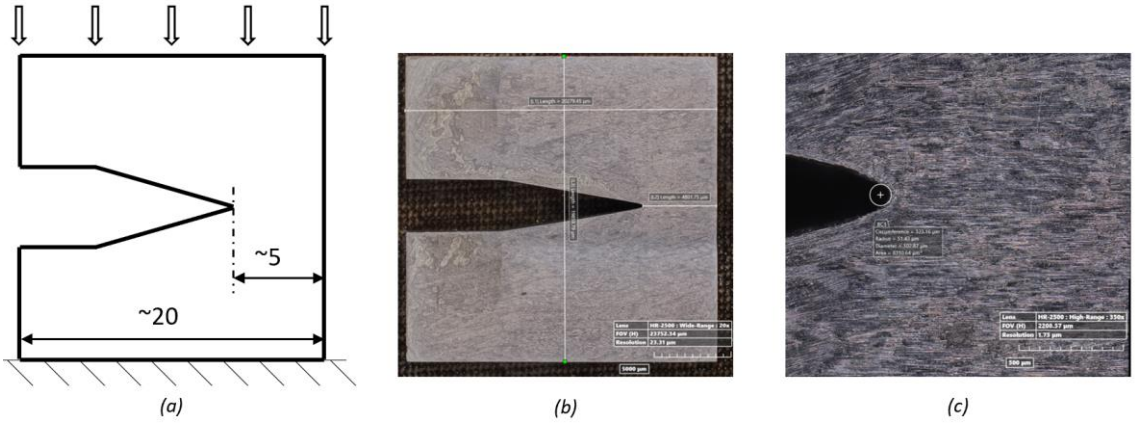

Figure 3. Small scale specimens manufactured: (a) nominal dimensions and loading scheme, (b) actual specimen microscopy with dimensions, (c) detail of the notch tip.

Table 3: Ligament dimensions and notch tip radii of the four specimens tested.

Specimen ID	Ligament length [mm]	Ligament thickness [mm]	Notch tip radius [µm]
BNF1	4.8	2.7	41
BNF2	4.8	2.7	51
FL1	4.9	2.9	43
FL2	4.8	2.9	48

2.4 Test method

The specimens were manually polished and gold coated. They were tested in compression, under displacement control, inside a Hitachi S-3700N SEM by means of a 5 kN in-situ loading stage from Deben UK. The displacement rate was set at 0.1 mm/min and data relative to jaws displacement and load were acquired at 10 Hz. The test was stopped at 400 N intervals to take SEM images of the specimen at different magnifications. The test was run either until complete failure of the specimen or up to a load of about 4.5 kN, in which case it was stopped to prevent damage to the load cell.

3. Results and discussion

The load-displacement curves for the specimens tested are reported in Figure 4. In these curves, small load drops correspond to relaxation occurring during the time the tests are stopped to take images. Both specimens containing foam strips, FL1 and FL2, did not fail by the end of the test. On the other hand, out of the two baseline specimens, BNF1 failed completely at a final load of about 3.83 kN, while specimen BNF2 did not fail by the end of the test.

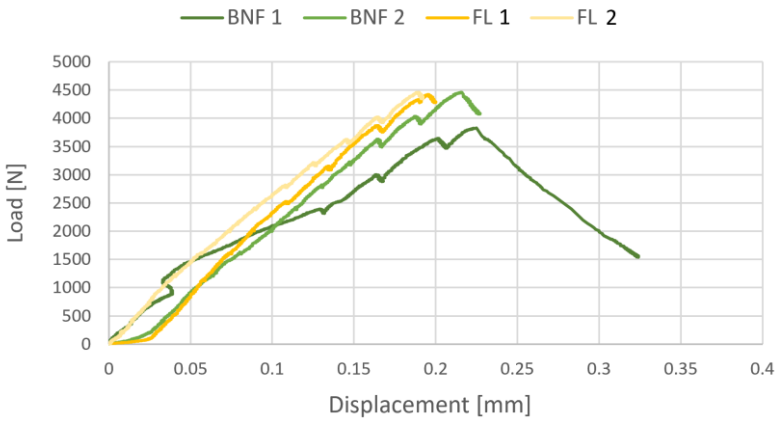

Figure 4. Load displacement curves for the four specimens tested.

Figure 5 shows SEM pictures of all specimens immediately before testing (Figure 5 (a)) and immediately after end of the tests (Figure 5 (b)). For all specimens, surface plies tended to delaminate from the rest of the specimen, and damage in the form of ply splits and fiber fracture is evident on them. By the end of the tests, for specimens BNF1 and BNF2, this damage extends from the notch tip all the way to the opposite specimen's side, and the superficial plies are completely delaminated in this region. In FL1 and FL2 specimens, the damage observed on surface plies is less extended: for FL1, it extends to about 2 mm away from the notch tip; for specimen FL2 a little amount of damage is observed extending from the notch tip toward the bottom side of the specimen.

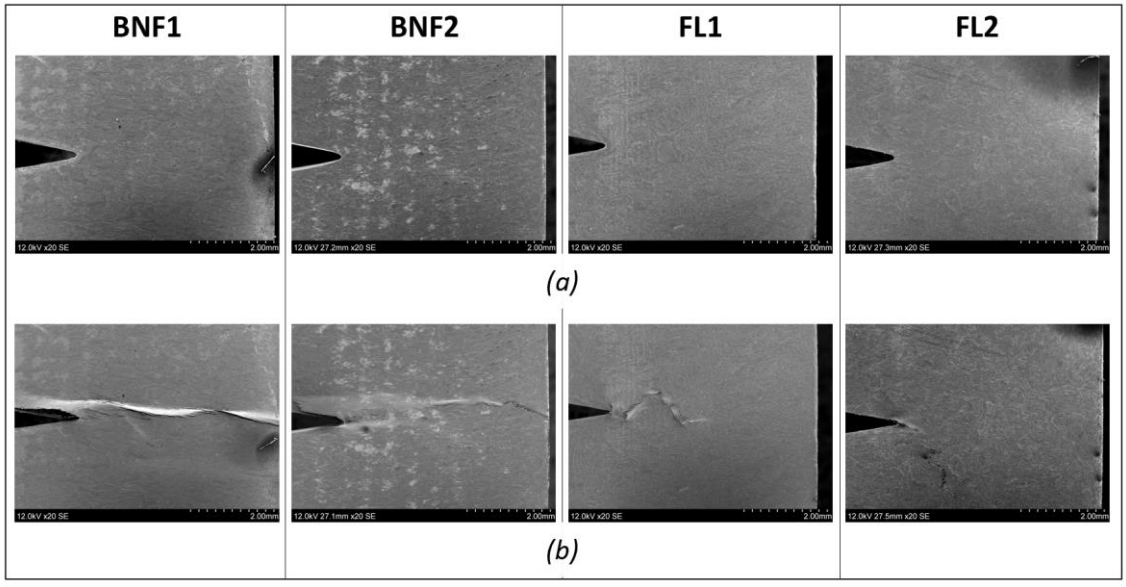

Figure 5. SEM pictures of the specimens' ligament (a) before testing and (b) right after the test.

Figure 6 shows X-ray images of the specimens after testing. One feature common to all the specimens is the presence of clear fracture lines emanating from the notch tip, at an angle of ±31°. The clarity with which these features are observed suggests that they might be somewhat continuous through the specimen thickness, for several layers. Considering the stacking sequence of the laminate (having ±31° ply blocks), it is hypothesized that these may have formed

by initial splitting of the layer with fiber orientation parallel to the direction of the fracture line and subsequent translaminar fracture of the layers with the opposite orientation. It is worth mentioning that X-ray images of FL1 and FL2 specimens show the striped pattern caused by the presence of the foam strips; these latter appearing darker in the images. From this it can be observed that, for both FL specimens, the tip of the notch is located in the middle of a dark region, that is in a region with foam strips.

Specimen BNF1, the only one that failed completely, shows a vast amount of damage going all the way from the notch tip to the opposite specimen's side. Damage probably consists mostly of kinkbands in 0° layers and translaminar fractures in ±31° layers. Additional splits at ±31° are also visible, as well as a wide delamination, as already seen from SEM observations. In specimen BNF2, a narrow damage band extends from the notch across almost the entire ligament length, accompanied by several splits, especially in the lower part of the specimen. Comparing this with BNF1, and considering that by the end of the test specimen BNF2 was still carrying a significant load, may suggest that the damage observed is limited to a few plies through the thickness, while most of the ±31° layers may still be intact and able to carry load. Delamination is also visible in the image, in an area enclosing all other damage observed. Specimen FL1 shows a similarly narrow band of damage extending for about 2.5 mm from the notch tip. An initial wider and brighter band cross a region without foam (lighter colored in the image); possibly this includes kinkbands in 0° layers and additional damage in other layers. As this band reaches the next region with foam strips (darker in the image), it divides into a 31° split, which then deviates into a -75° split, and an almost horizontal narrower band. These two narrow bands then reach the beginning of the next region without foam, where they arrest. Interestingly, specimen FL2 shows no damage at all, except for the already mentioned fracture lines originating from the notch tip. It is likely that these fracture lines and the foam strips present at the notch tip have acted as strong blunting factors, preventing significant stress concentration and damage initiation and propagation from the notch altogether.

Additional fractographic activities will help to fully understand the fracture behavior of the specimens.

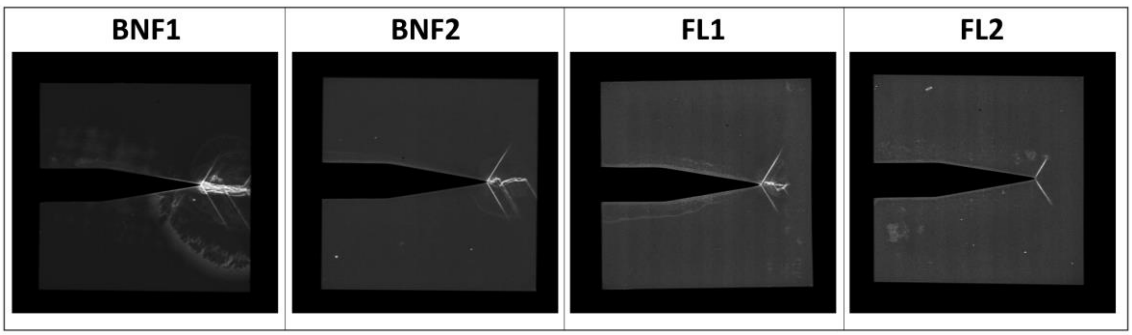

Figure 6. X-ray scans of the four tested specimens.

4. Conclusions

The study presented is concerned with the preliminary design, manufacturing and testing of a bioinspired microstructure for MD CFRP laminates aiming at mitigating compressive failure.

After designing a suitable configuration, a tailored procedure for manufacturing of the desired microstructure was developed. The procedure features adoption of laser cutting for the preparation of the composite prepreg and of the foam sheets used for creating the soft inclusions. Additionally, PET sheets are adopted to create templates for precise positioning of the two former components, with alignment being ensured by means of a system of alignment pins. The developed procedure allows precise manufacturing of the microstructure. In-situ tests were performed on four small scale notched specimens, two baseline ones and two containing soft inclusions. After the tests, X-ray imaging of the specimens was performed to gain a deeper understanding of the specimens' behavior. Out of the four specimens tested, only one baseline specimen failed completely; other tests had to be stopped to avoid damage to the rig's load cell. Our results suggest that splitting and translaminar fracture in off-axis plies from the notch tip occurred and acted as a strong crack blunting mechanism, reducing the stress concentration and the propensity to fracture initiation and propagation from the notch. While the results shown have to be expanded on further experimental activities, it was observed that specimens containing the soft inclusions had a reduced amount of damage when compared to baseline.

Further activities are underway to gain a deeper understating of the results obtained and produce further results to assess the effectiveness of the microstructure designed.

Acknowledgements

The authors kindly acknowledge the funding for this research provided by UK Engineering and Physical Sciences Research Council (EPSRC) programme Grant EP/T011653/1, Next Generation Fibre-Reinforced Composites: a Full Scale Redesign for Compression in collaboration with University of Bristol.

YoneshimaFelt Co. Ltd. and the person of Tomoya Yoneshima are kindly acknowledged for providing PMI foam sheets used for this research.

5. References

1. Pinho ST, Iannucci L, Robinson P. Physically-based failure models and criteria for laminated fibre-reinforced composites with emphasis on fibre kinking: Part I: Development. Composites Part A: Applied Science and Manufacturing 2006; 37:63-73.
2. Tsampas SA, Greenhalgh ES, Ankersen J, Curtis PT, On compressive failure of multidirectional fibre-reinforced composites: A fractographic study. Composites Part A: Applied Science and Manufacturing 2012; 43:454-468.
3. Kolednik O, Predan J, Fischer FD, Fratzl P. Bioinspired Design Criteria for Damage-Resistant Materials with Periodically Varying Microstructure. Advanced Functional Materials 2011; 21:3634-3641.
4. Rohacell® SL datasheet, accessed on 19/04/2022. https://www.rohacell.com/product/peek-industrial/downloads/rohacell%20sl_2020_january.pdf

